Study of the role of latent heating in upper-level cold-core low formation during the mei-yu season

Wang, Mark Yin-Mao and Chen, George Tai-Jen

Atmospheric Sciences, National Taiwan University, Taipei, Taiwan

Kuo, Bill Ying-Hwa

National Center for Atmospheric Research, Boulder, Colorado, USA

November 4, 2010

Definition:

Two types of CCL (Tsay 1998, Kuo 1998, Chou 1989, Chen et al. 1988, 1989) or cold-vortex (Chen and Chou 1994):

1. Palmén type (Palmén 1949, Hoskins 1985): Originates (cuts-off) from mid-latitude synoptic scale trough, and often moves eastward.

2. Palmer type (Palmer 1953) (or TUTT cells): Originates from easterly trough near the southern edge of subtropical high, or at the neutral point in a saddle field, often moves westward.

Paper review:

- Tang (2000), Chen & Tang (2004): Palmer type Hailstorm over northern Taiwan on 2 July 1998

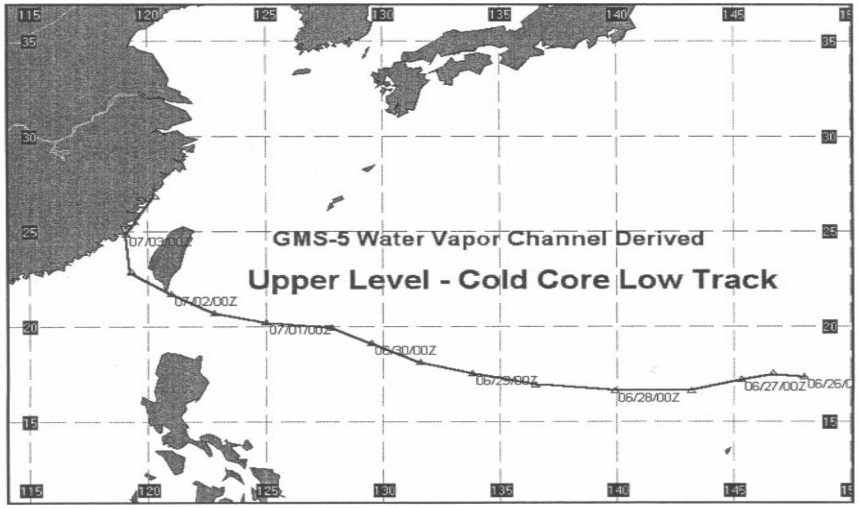

圖4.2　1998年6月26日0000 UTC～7月3日1200 UTC，GMS-5水氣頻道衛星雲圖追蹤所得的高層冷心低壓中心路徑，"Δ"為每隔12小時之中心位置。

1. CCL circulation increased vertical shear
2. CCL thermal structure enhanced convective instability
3. Upper-level divergence favored for convection through a jet streak of the CCL

Paper review:

Bosart et al. (1991):

- Tropical storm formation in a baroclinic environment
- CCL provided initial cyclonic circulation at middle to high troposphere
- Ascent motion ahead of the CCL

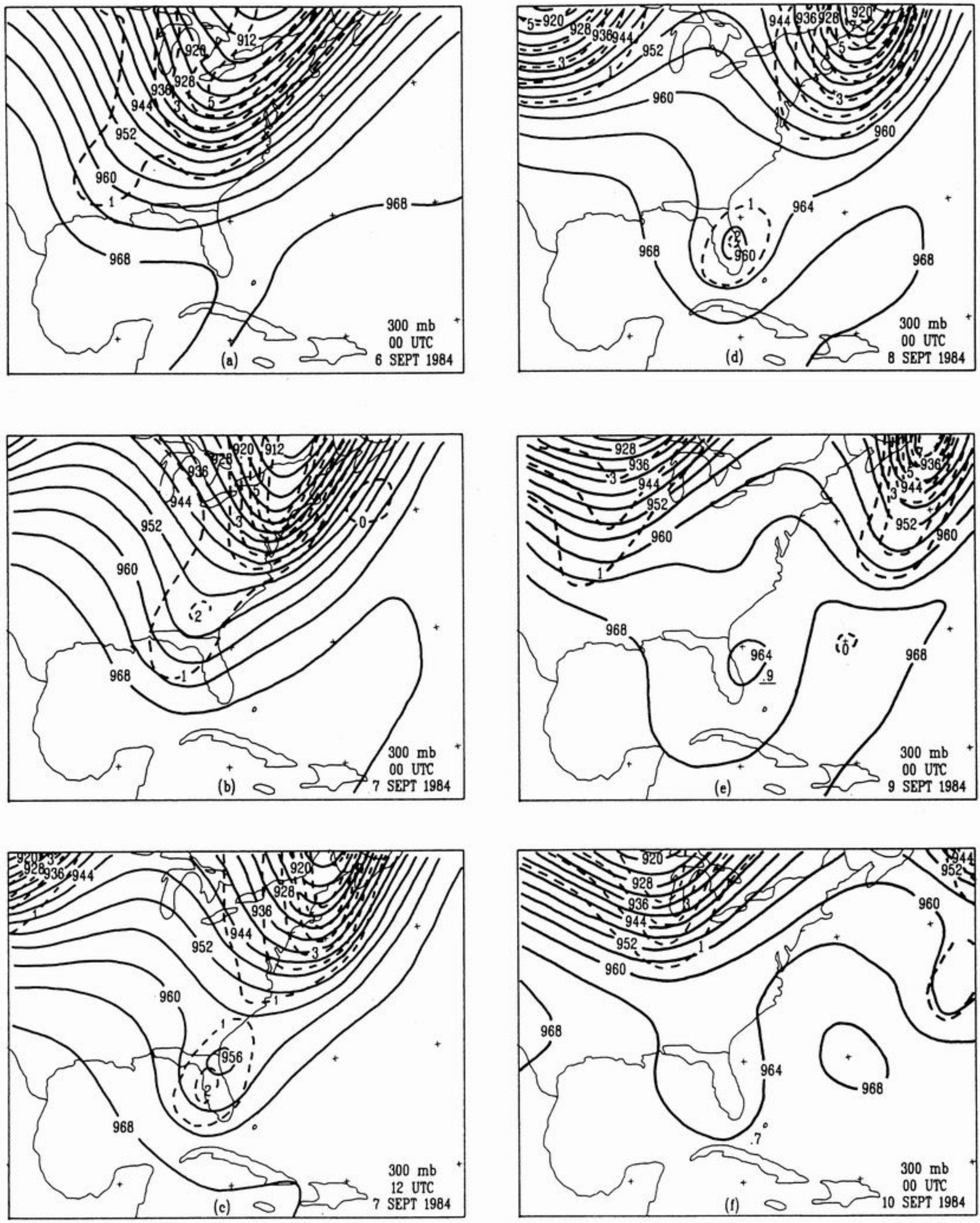

FIG. 19. Geopotential heights (solid) at 300 mb every 4 dam and potential vorticity (dashed) every 1.0 × 10^{-6} K kg^{-1} m^2 s^{-1} at 300 mb for: (a) 0000 UTC 6 September 1984; [(b), (c)] 0000 UTC and 1200 UTC 7 September 1984; [(d)–(f)] 0000 UTC 8–10 September 1984.

Climatological pattern of COL:

EC_2.5°×2.5°, 1994~2008

NMC_2°E×5°N, 1963~1977

Bell and Bosart (1989)

1994~2008 spring 500 hPa COL

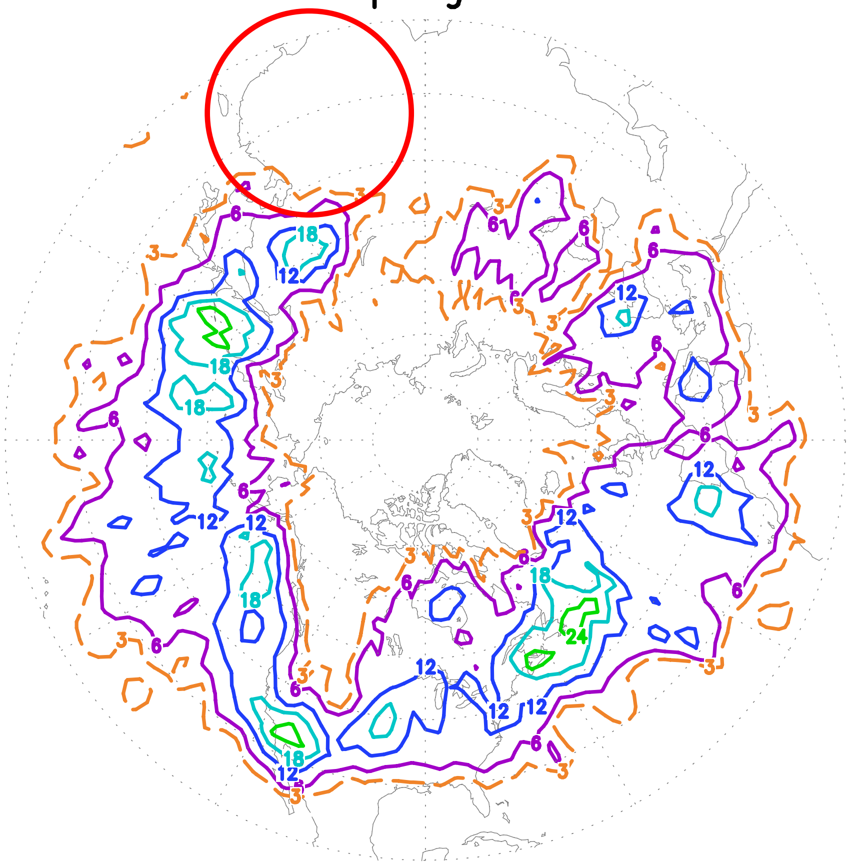

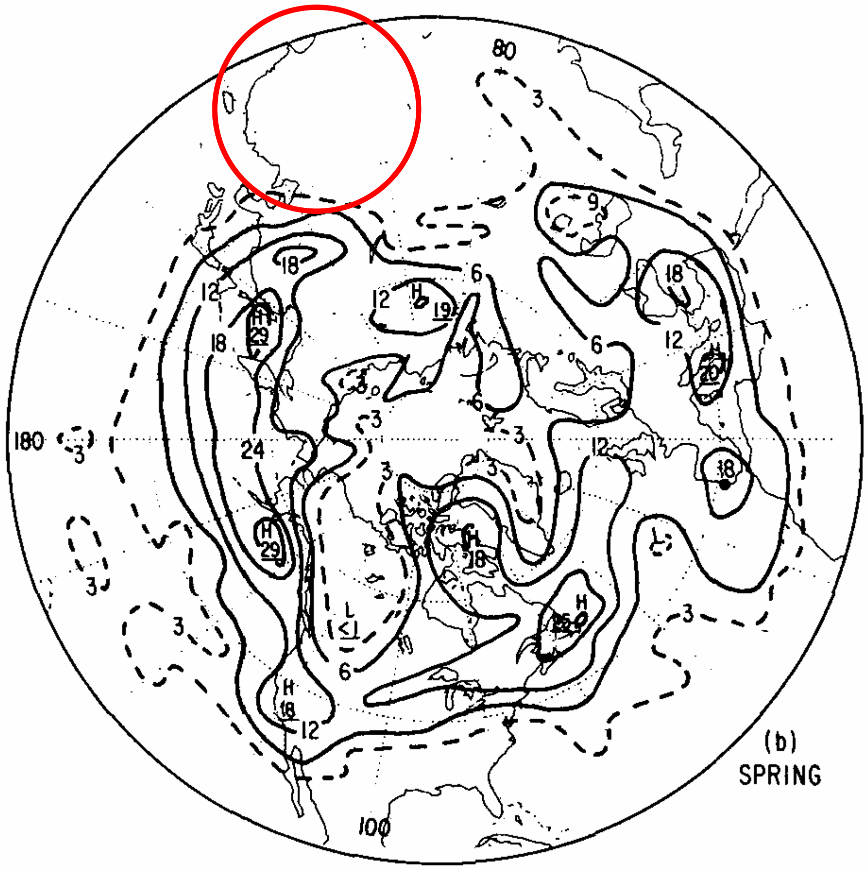

Case briefing: Tsay (1998), Santurette et al. (2005)

CCL can be found in WV channel.

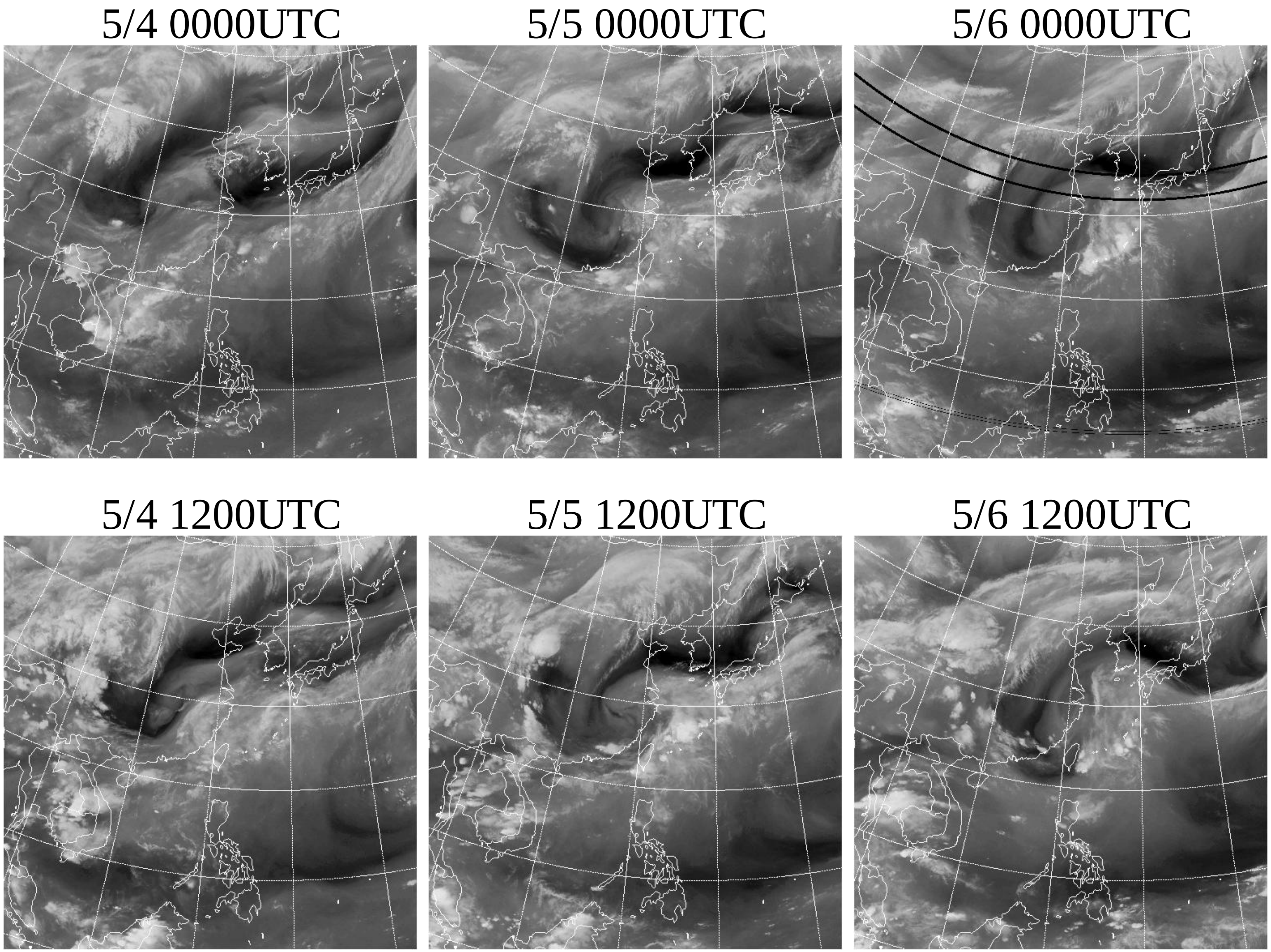

Case study:

(a) 1998 5/3 0600 UTC

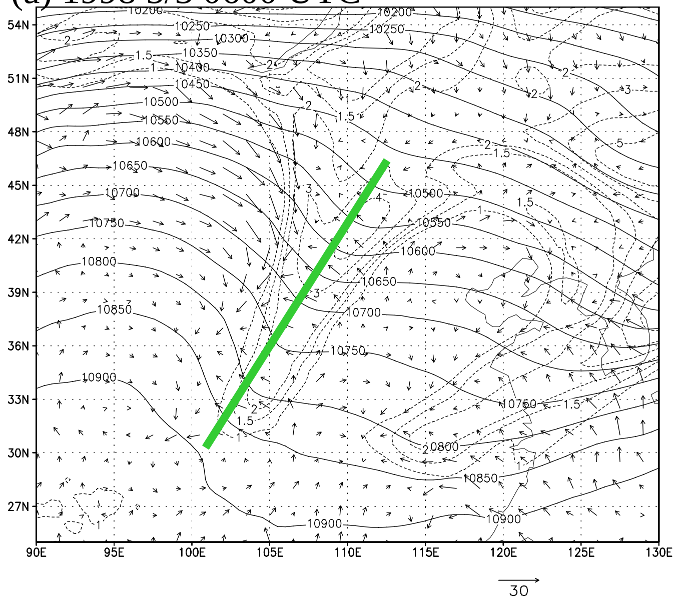

(c) 1998 5/5 0000 UTC

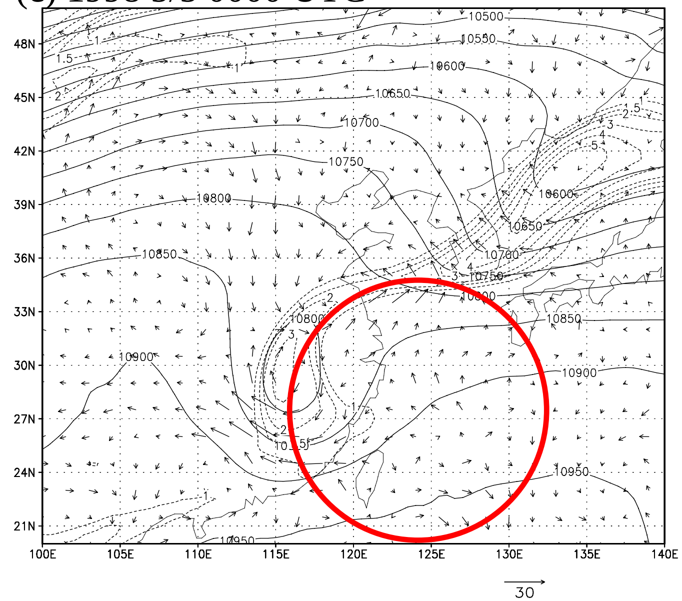

(b) 1998 5/4 0600 UTC

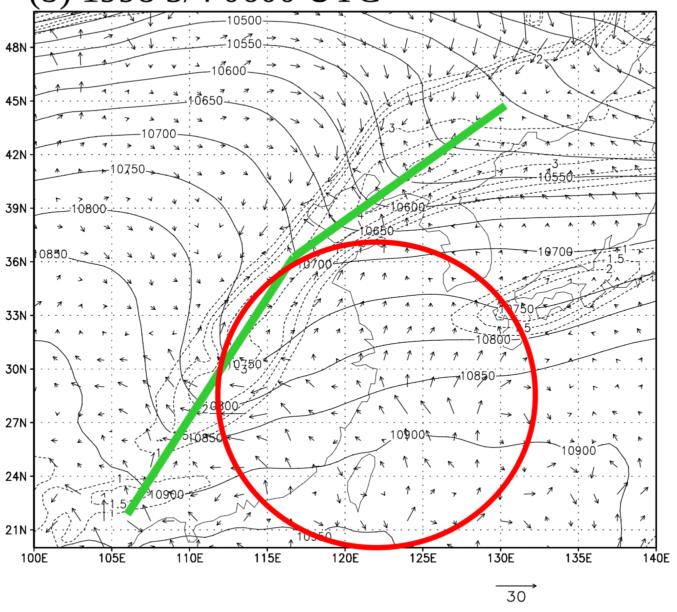

98 May4 06Z 250hPa Z(m), Vag(m/s) and PV(PVU)

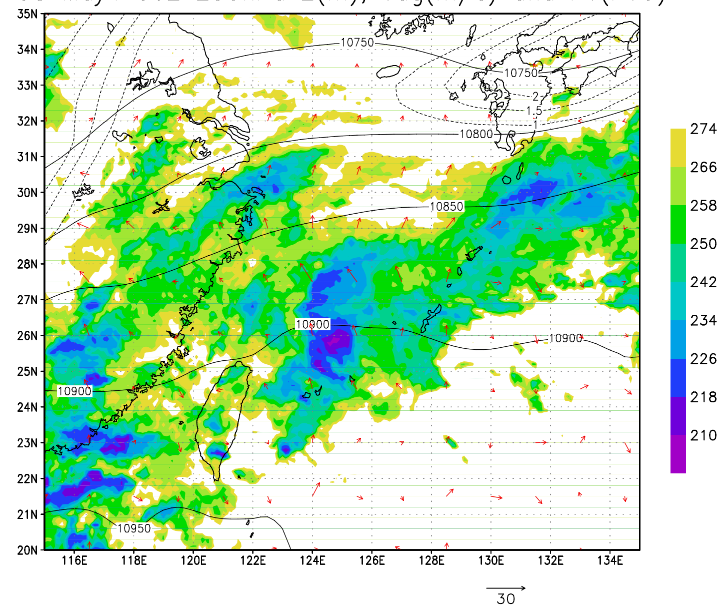

Paper review: Keyser and Shapiro (1986)

Confluence trough
→upper level frontogenesis, jet formation and intensification

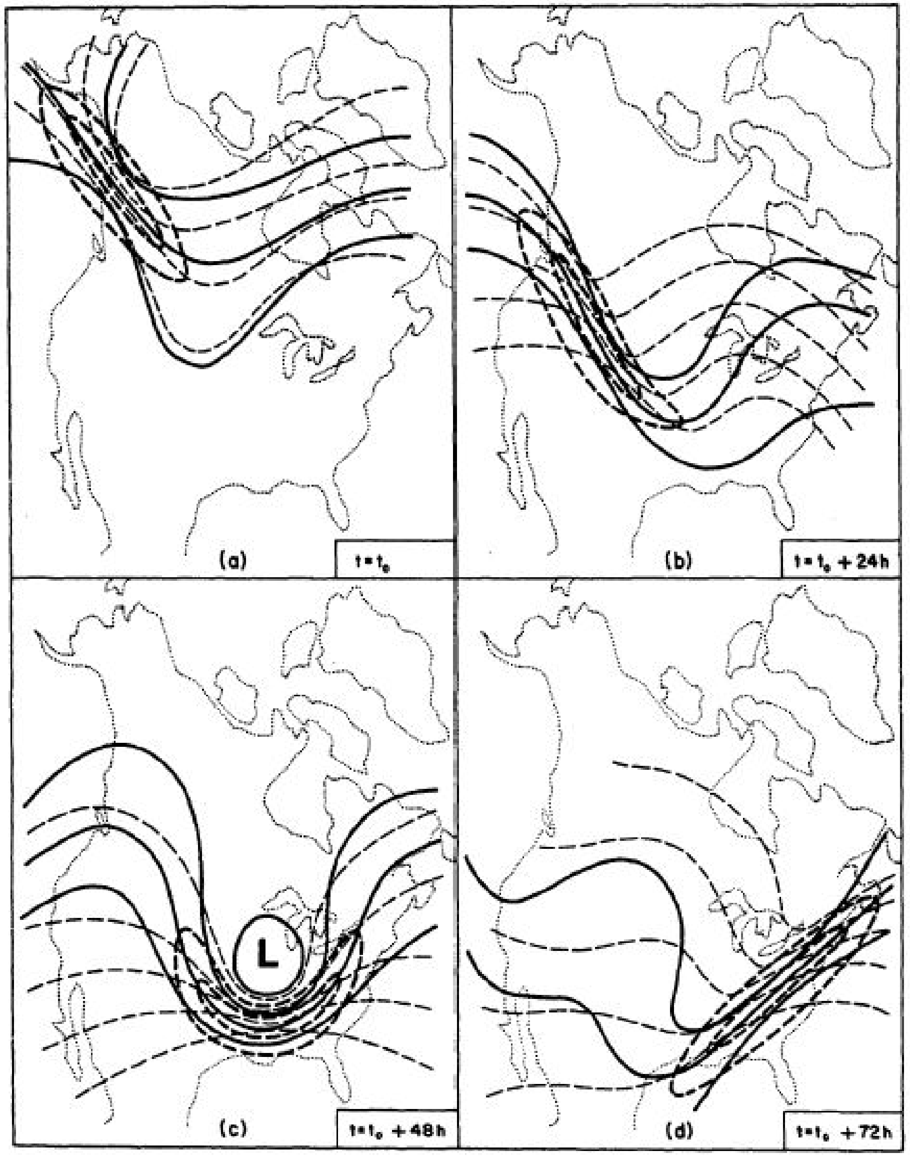

NW-SE tilt trough
→barotropic amplification
Thermal wave lags height wave
→baroclinic amplification

Symmetric pattern (no tilt, no lags)
→the cessation of barotropic and baroclinic amplification

NE-SW tilt trough
→barotropic damping
Thermal wave leads height wave
→baroclinic damping

Paper review: Bell & Keyser (1993)

$$\mathrm{PV} = \frac{1}{\sigma}\left(f + V\frac{\partial \alpha}{\partial s} - \frac{\partial V}{\partial n} \right)$$

$$= \mathrm{PV}_{cu}(\text{trough}) + \mathrm{PV}_{sh}(\text{jet})$$

overlap

A cut-off low formed

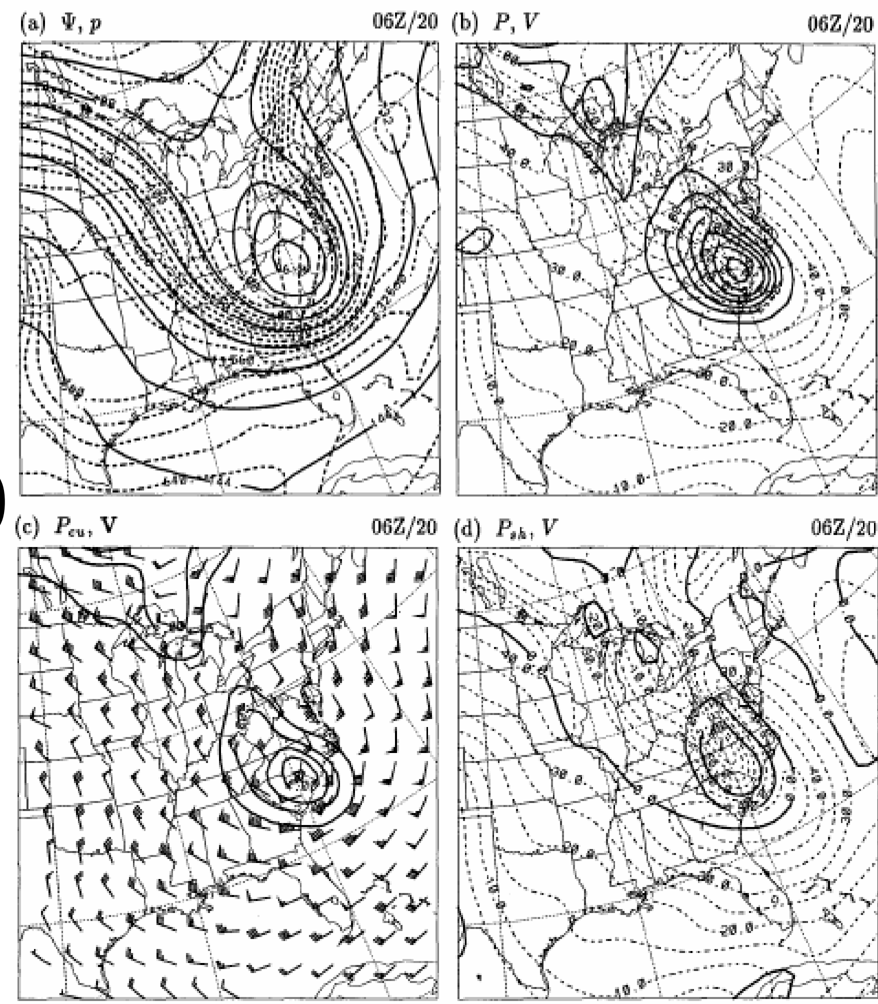

FIG. 10. As in Fig. 4 except for 0600 UTC 20 January 1986.

Paper review:

- Thorncroft, Hoskins and McIntyre (1993)

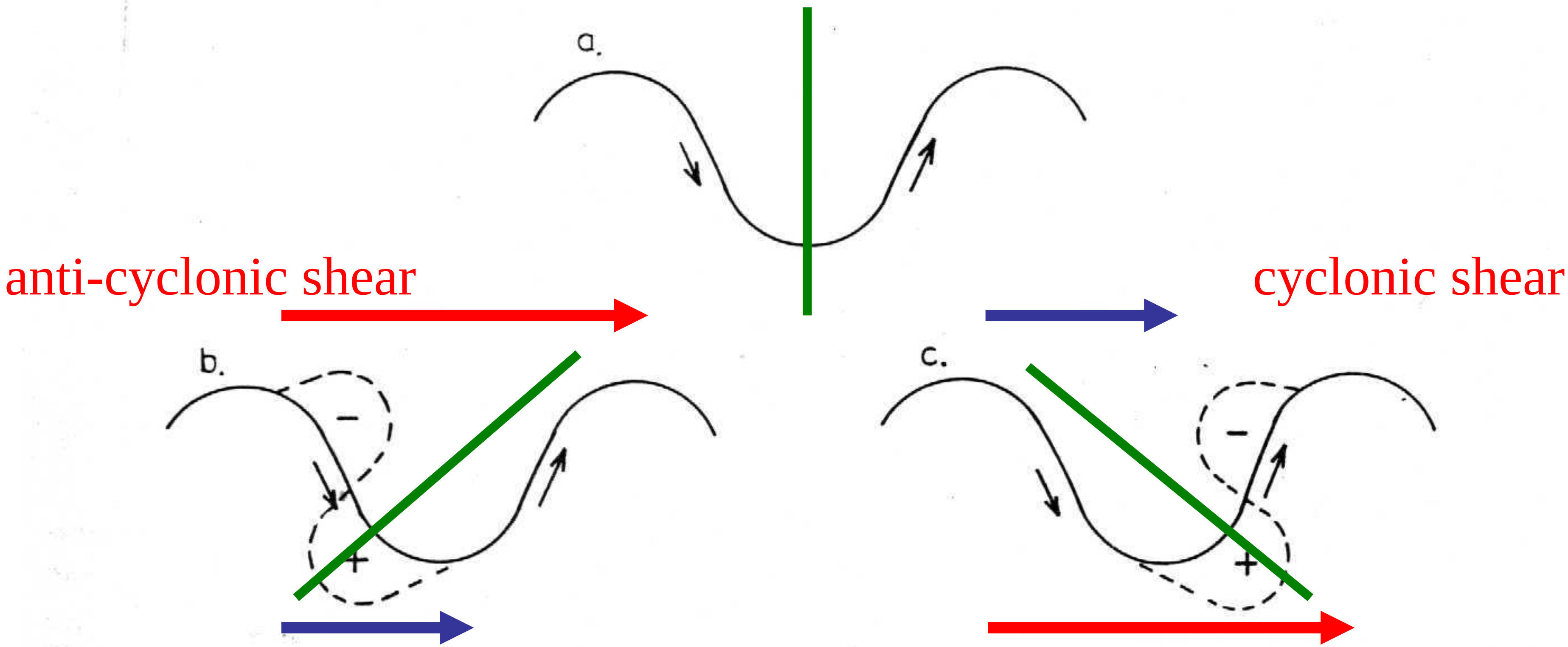

Figure 13. A thought experiment indicating the effects of meridional shear on the evolution of an initially sinusoidal PV-theta contour: (a) indicates a contour with implied winds before the meridional wind shear has tilted it. The dashed contours in (b) and (c) represent the configuration resulting from anticyclonic or cyclonic tilting, respectively (see text).

Case study: TRMM (Huffman et al. 2007)

precipitation radar

Precip.

1998 5/4

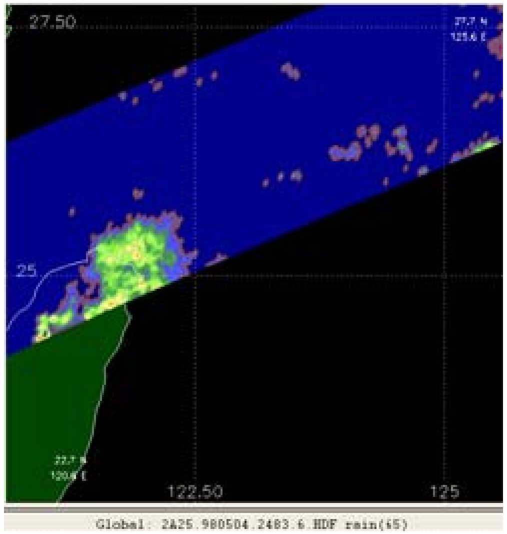

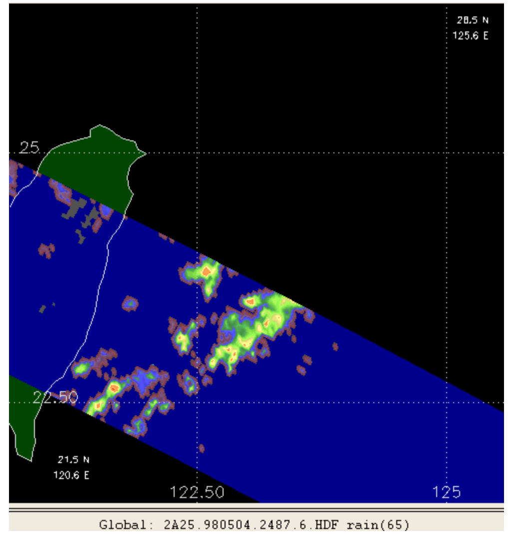

5/4 0300 UTC

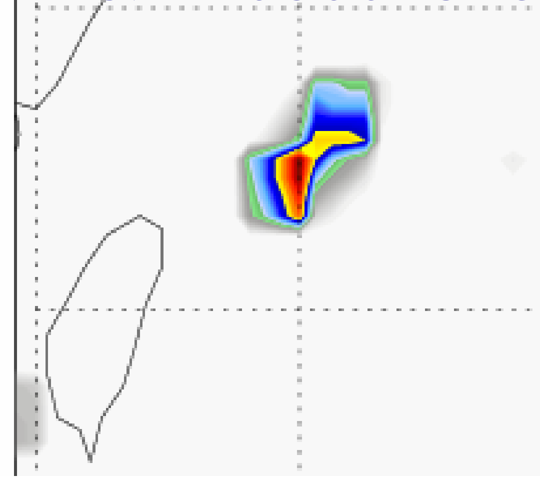

1998 5/5

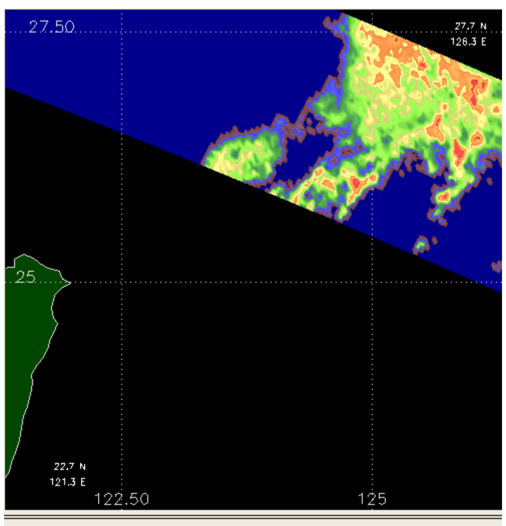

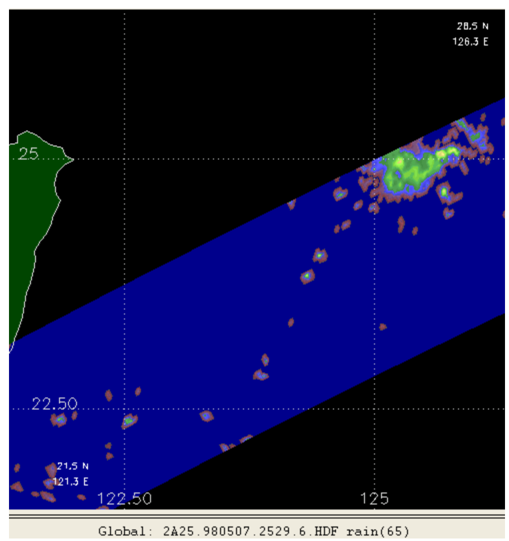

5/4 0600 UTC

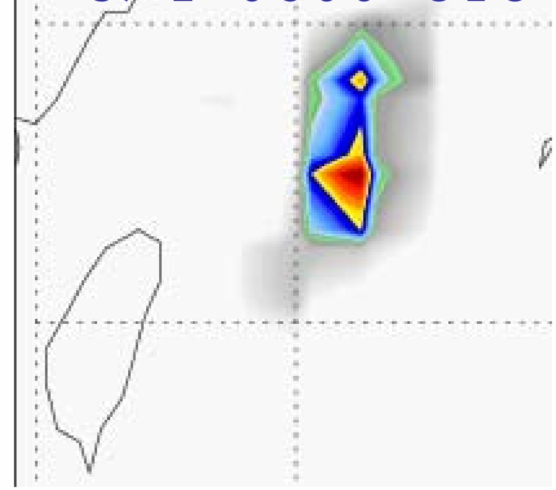

Case study: observation

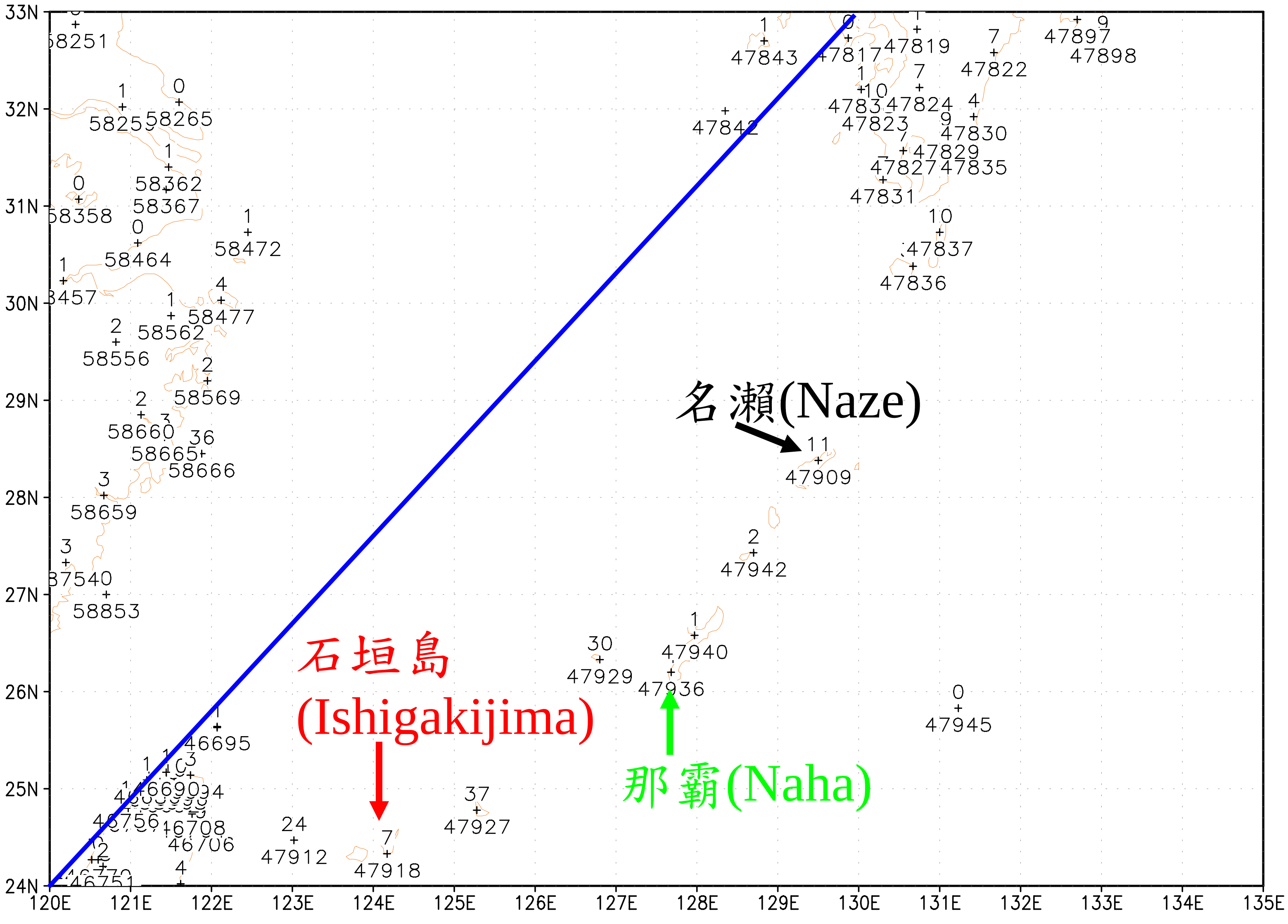

Case study: observation

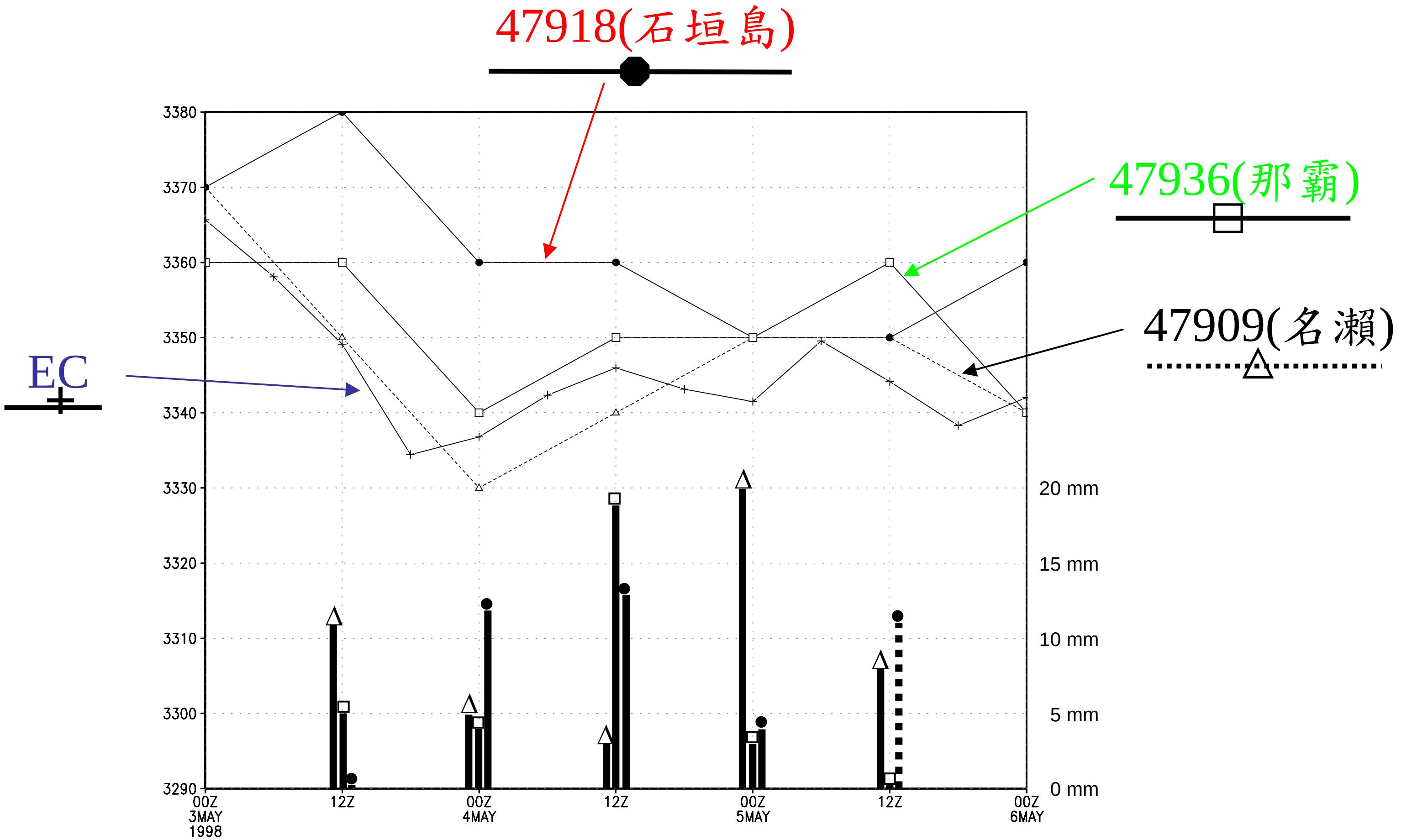

Fig. 12 Thickness of 250 to 400 hPa (gpm) of 47918 (solid line with filled circle), 47936 (solid line with opened square), 47909 (dash line with triangle) and EC averaged (solid line with cross). Also shows 3-hour rainfall (mm, bars), from left to right are 47909(Δ), 47936(□), and 47918(●), respectively. The rainfall of 47918 (solid dash line)at 1200 UTC 5 May lacked, and here interpolate by 0000 UTC 5 and 6 May.

Case study: Cross section PV anomaly

PV average: 40 times + zonal(70°E~170 °E)

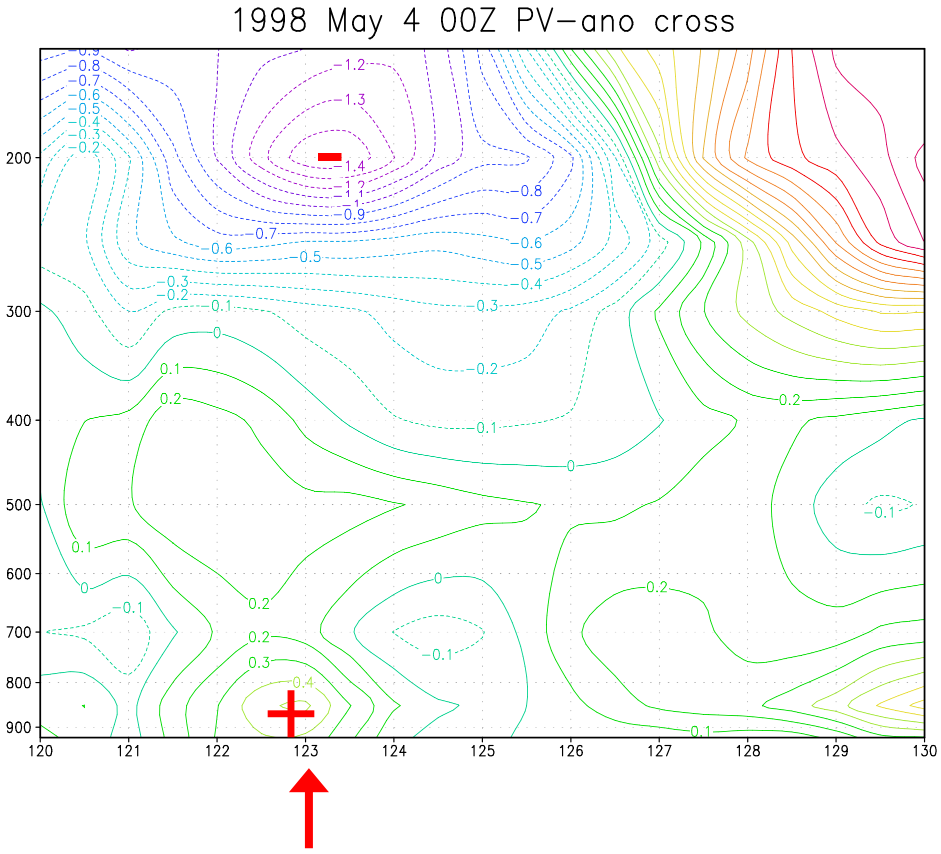

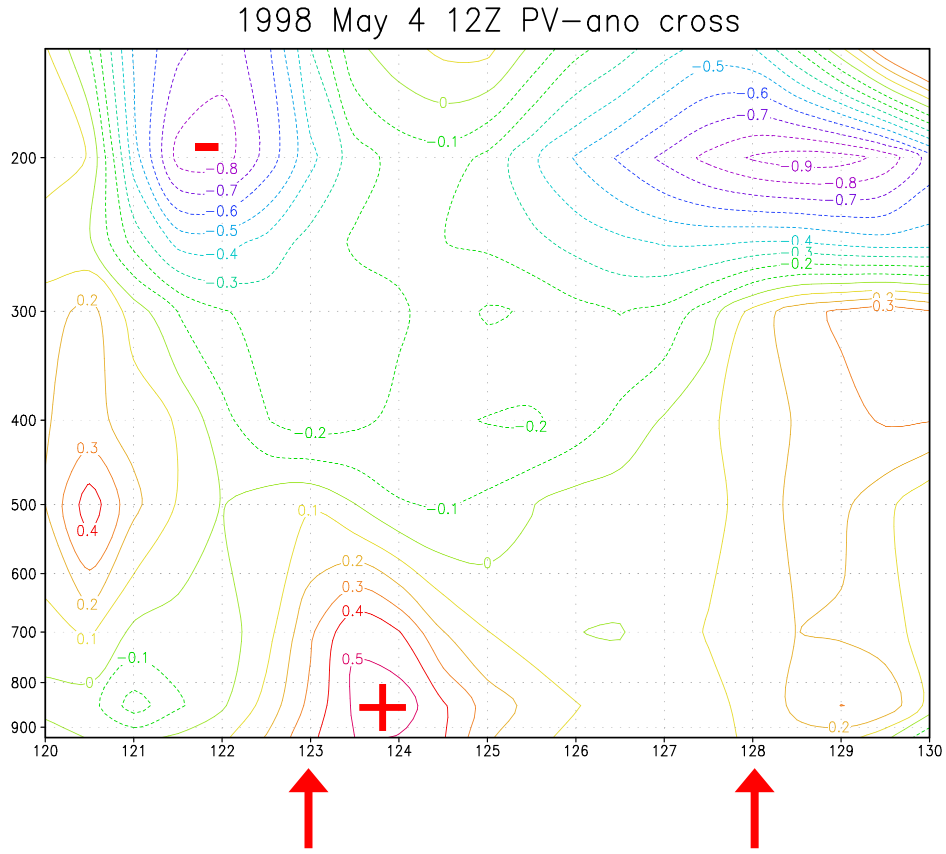

Case study: Q1 & Q2 at 5/4 0600UTC 1998

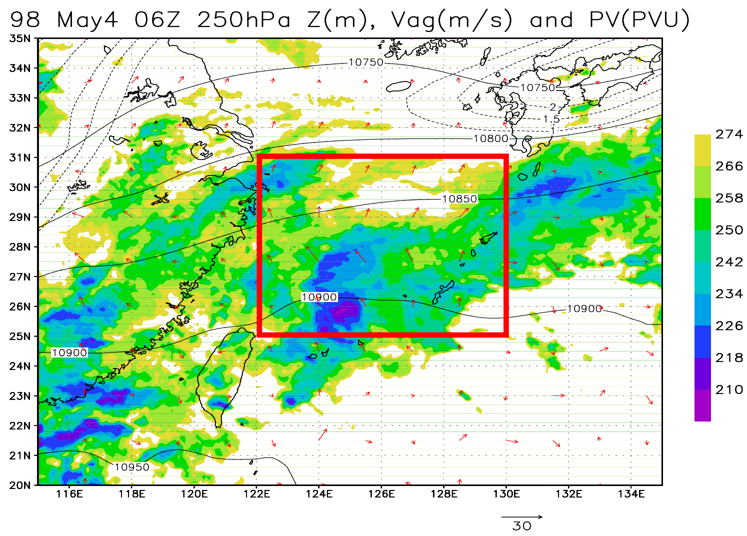

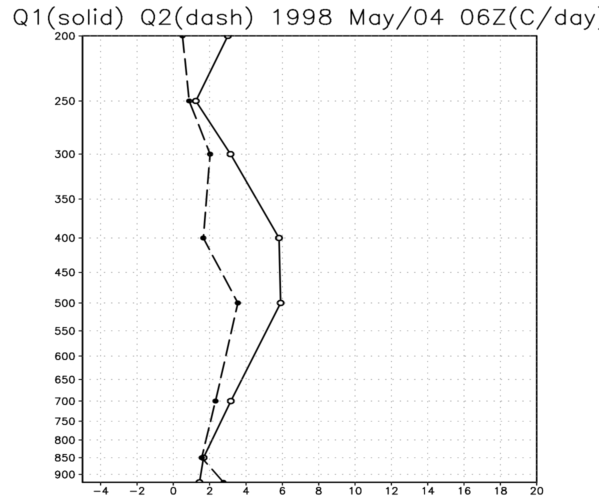

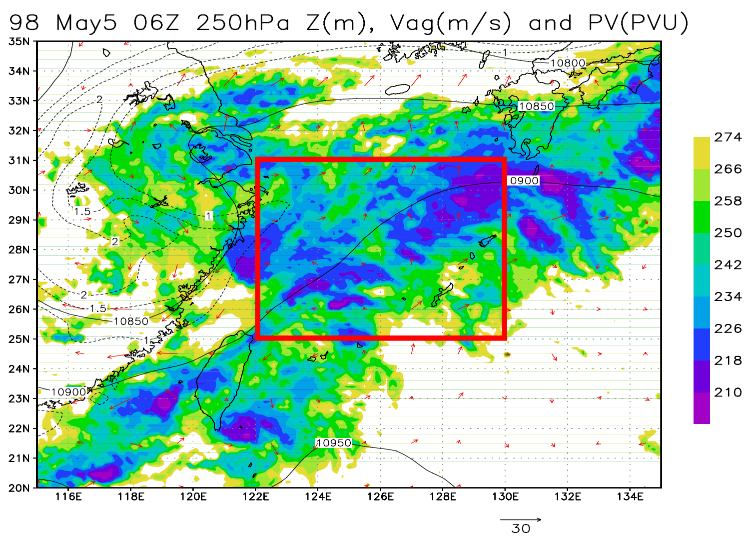

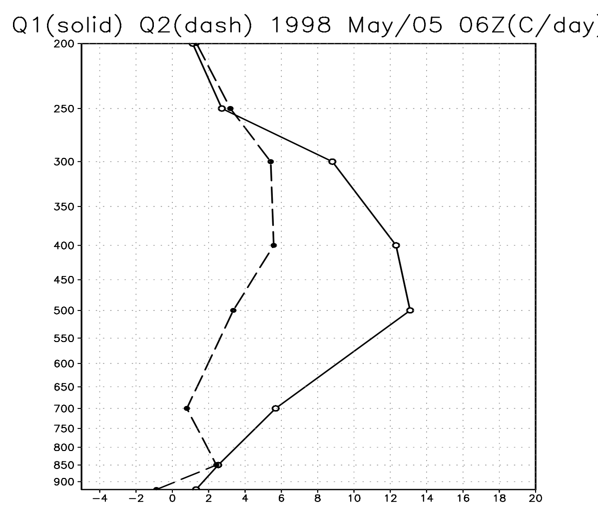

MM5: Initial time: 00Z, 4 May 1998, CTRL vs. FDRY

5/05 00Z 250 hPa Z CTRL(solid) vs. FDRY(dashed)

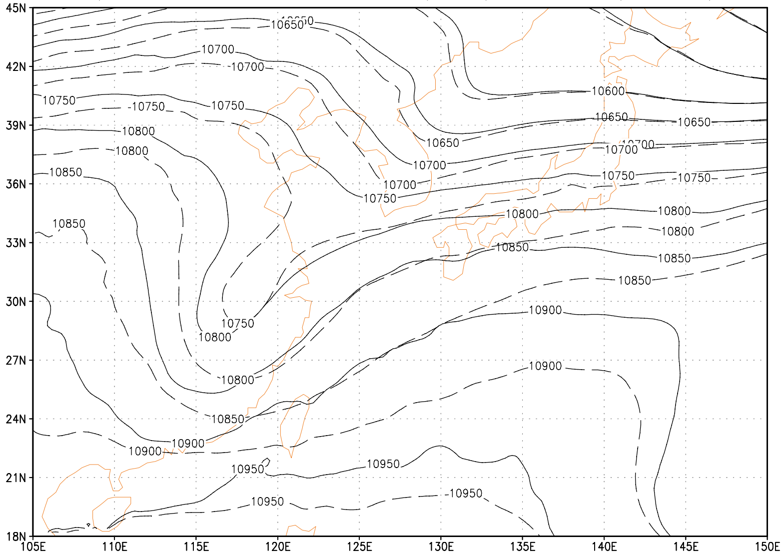

5/06 00Z 250 hPa Z CTRL(solid) vs. FDRY(dashed)

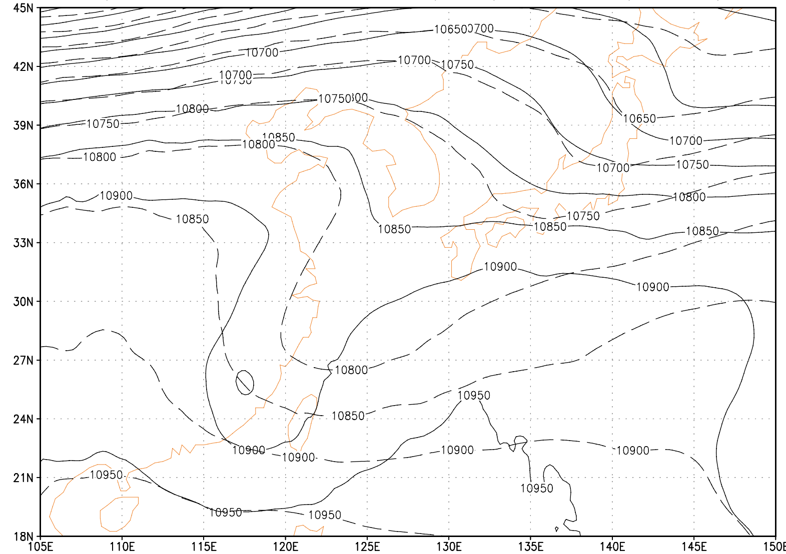

5/05 12Z 250 hPa Z CTRL(solid) vs. FDRY(dashed)

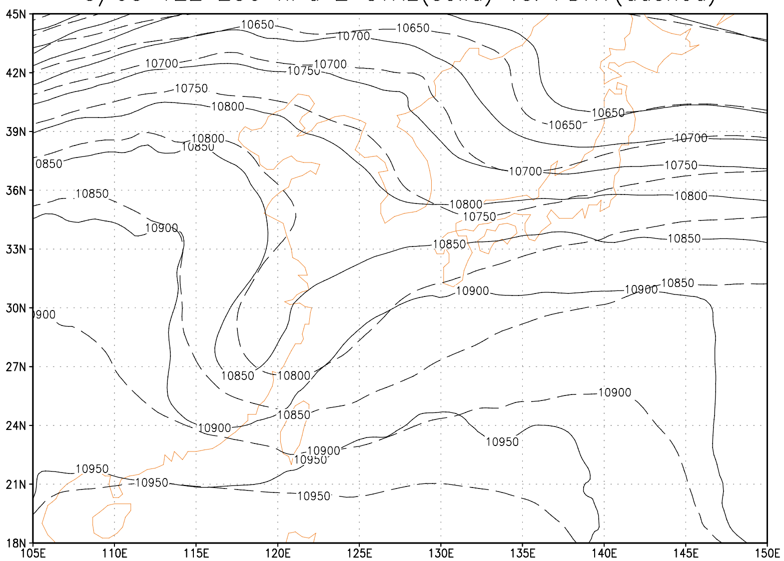

5/06 12Z 250 hPa Z CTRL(solid) vs. FDRY(dashed)

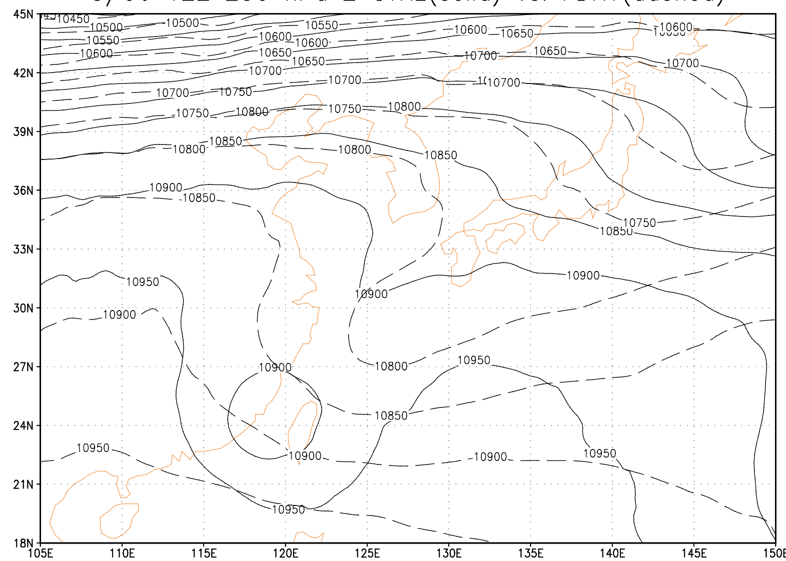

Paper review:

- Thorncroft, Hoskins and McIntyre (1993)

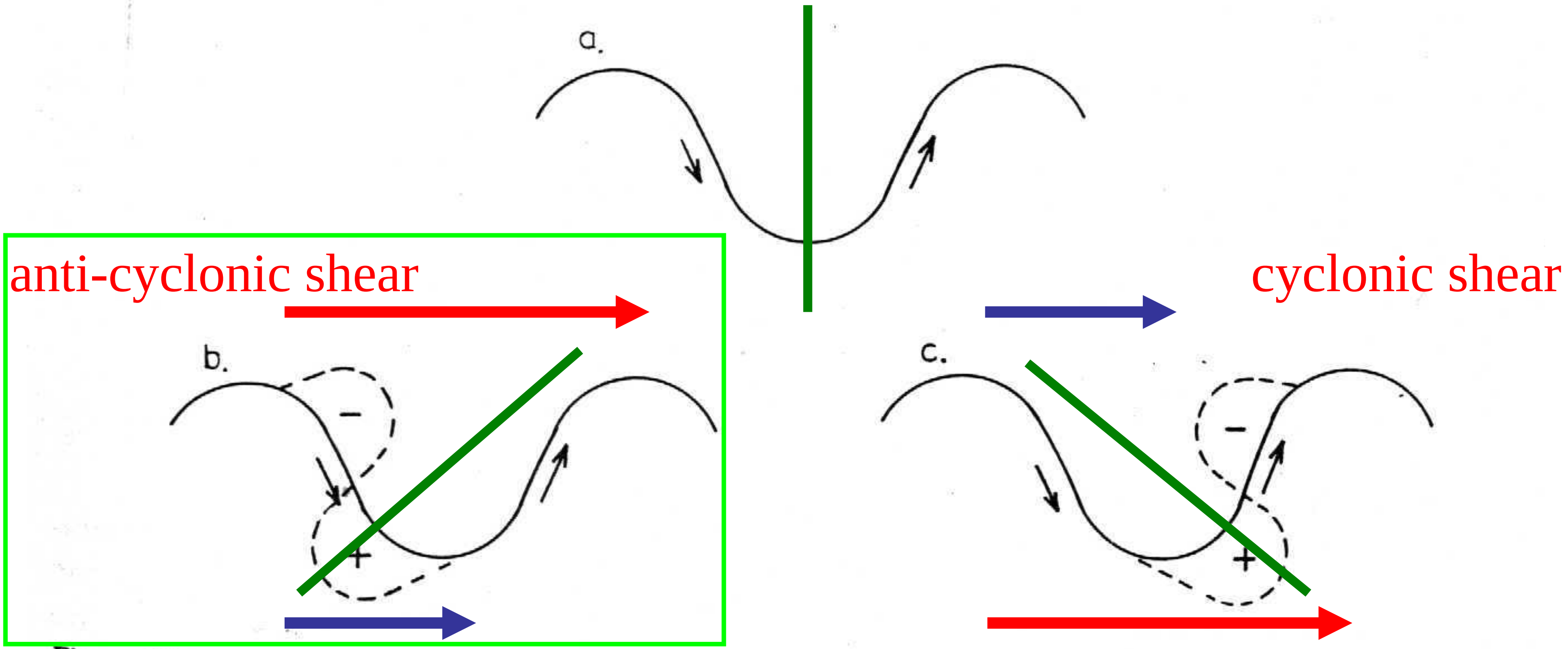

Figure 13. A thought experiment indicating the effects of meridional shear on the evolution of an initially sinusoidal PV-theta contour: (a) indicates a contour with implied winds before the meridional wind shear has tilted it. The dashed contours in (b) and (c) represent the configuration resulting from anticyclonic or cyclonic tilting, respectively (see text).

MM5: Initial time: 00Z, 4 May 1998, H CTRL-FDRY, dBZ

5/05 00Z 250 hPa Z CTRL-FDRY

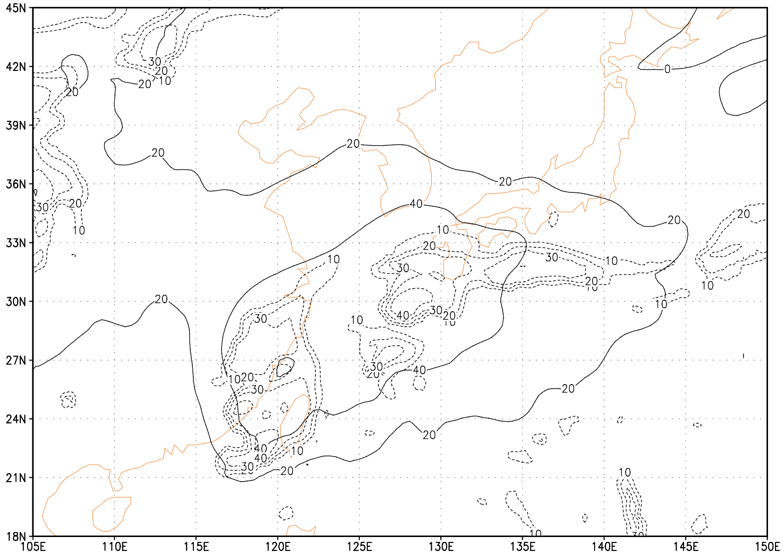

5/06 00Z 250 hPa Z CTRL-FDRY

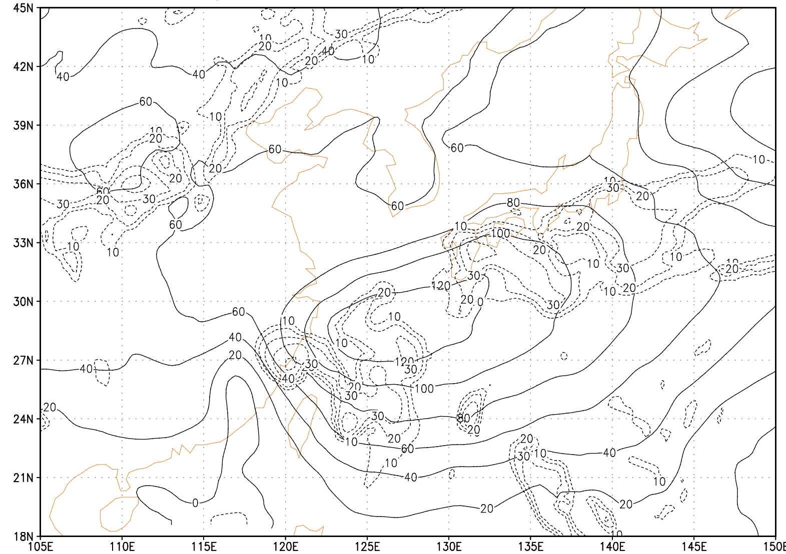

5/05 12Z 250 hPa Z CTRL-FDRY

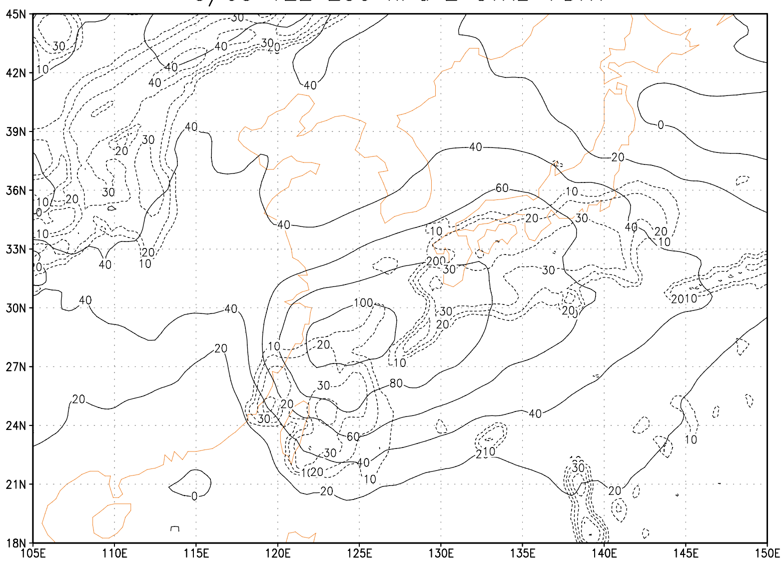

5/06 12Z 250 hPa Z CTRL-FDRY

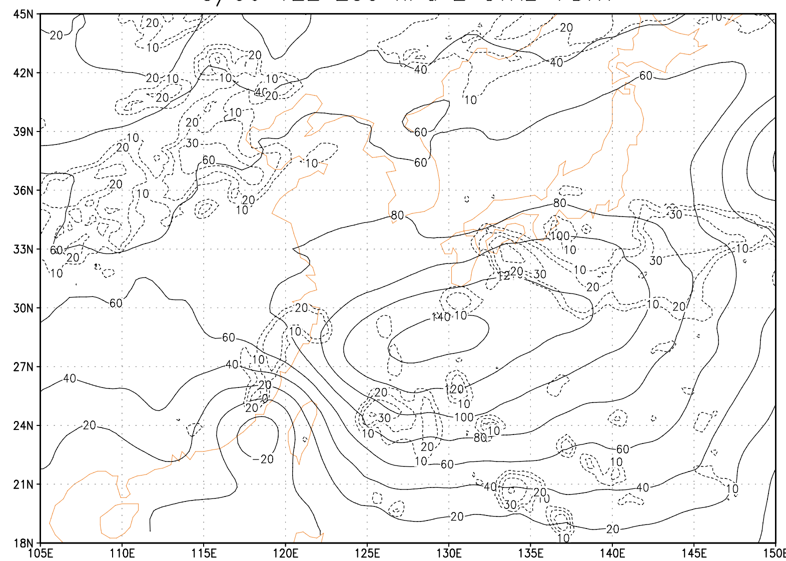

Paper review: Postel and Hitchman (1999, 2001)

Rossby Wave Breaking (RWB) along the subtropical tropopause

By the linear dynamical framework, the two-dimensional Rossby wave dispersion relationship in linearized QGPV equation in barotropic flow:

$$c_x - \overline{u} = -\overline{q}_y (k^2 + l^2)^{-1}, \qquad (1)$$

c_x : phase speed of wave in zonal direction

$\overline{u}$: zonal velocity with varying latitudinally

$\overline{q}_y$: meridional gradient of mean QGPV

k : zonal wavenumbers of disturbance

l : meridional wavenumbers of disturbace

Paper review: Stoelinga (1996)

"Not all of the irrotational wind field can be attributed to latent heating, but its effect is clearly to enlarge the warm tropopause region (or ridge)."

"It helps to keep the upper wave structure phase locked with the surface disturbance."

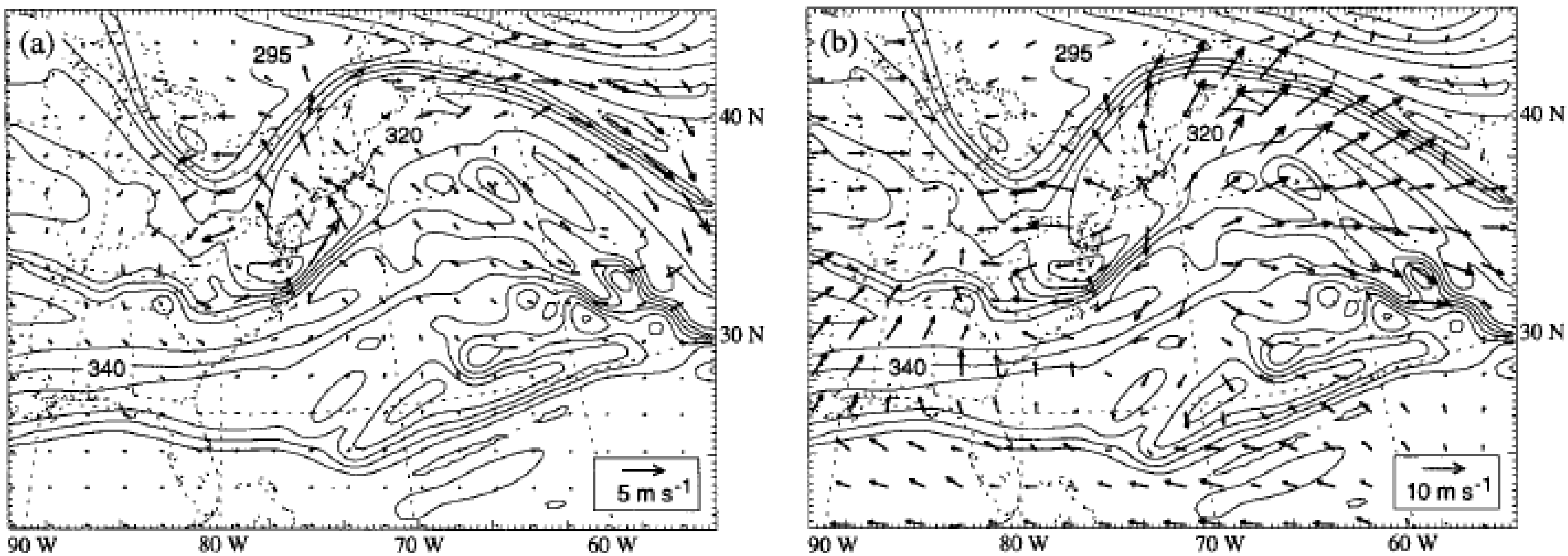

FIG. 14. The 24-h (1200 UTC 23 February) tropopause-level (PV = 1.5 PVU) potential temperature (contour interval 2 K) with tropopause-level vector wind fields (scale at lower right): (a) balanced winds from PV and surface potential temperature generated by explicit latent heating (q_{lh} and θ_{lh} in text); (b) irrotational wind. Note different vector scales in (a) and (b).

Summary

1. Statistically study shows the rare appearance of COL at East Asia.

2. The structural characteristics of this Palmén type CCL is similar to the Palmer type.

3. Before the trough bent, its evolution can be explained by adiabatic process as proposed by Thorncroft et al.(1993).

Summary

4. Diabatic heating process plays a key role in the cut-off process of this case.

   Kinematically, the convection blocked eastward movement of southern portion of the trough.

   Dynamically, the trough encountered RWB condition (critical layer) through the appearance of upper-level easterly by convection. ($C_x - u \rightarrow 0$)

Thanks you!

Climatological pattern of COL:

EC_2.5°×2.5°, 1994~2008

NMC_2°E×5°N, 1963~1977

Bell and Bosart (1989)

1994~2008 summer 500 hPa COL

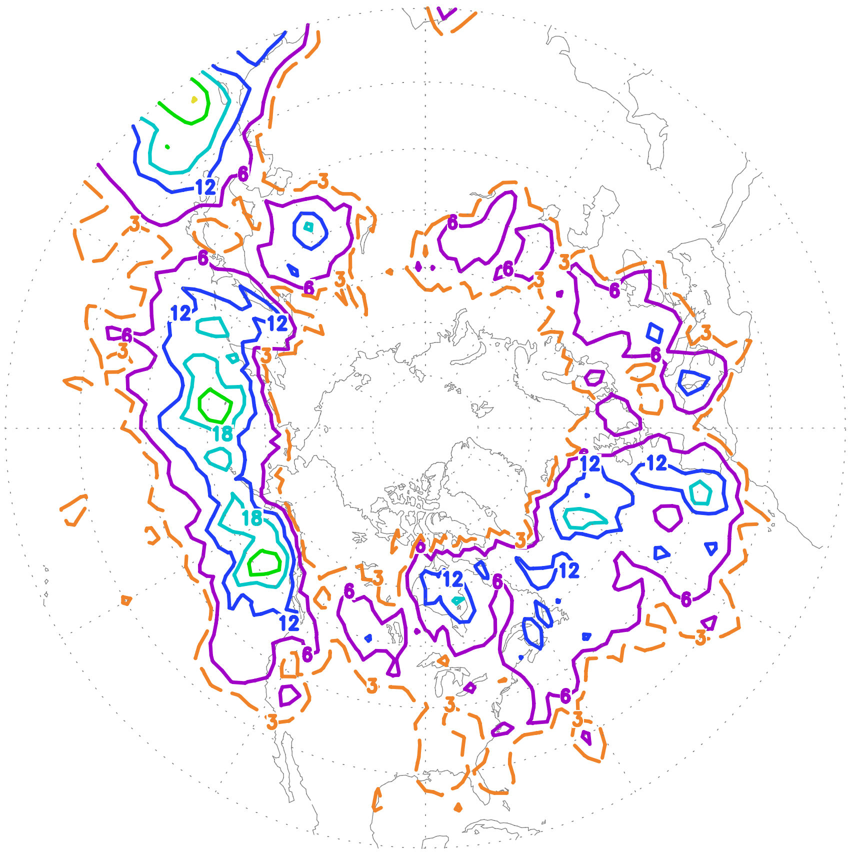

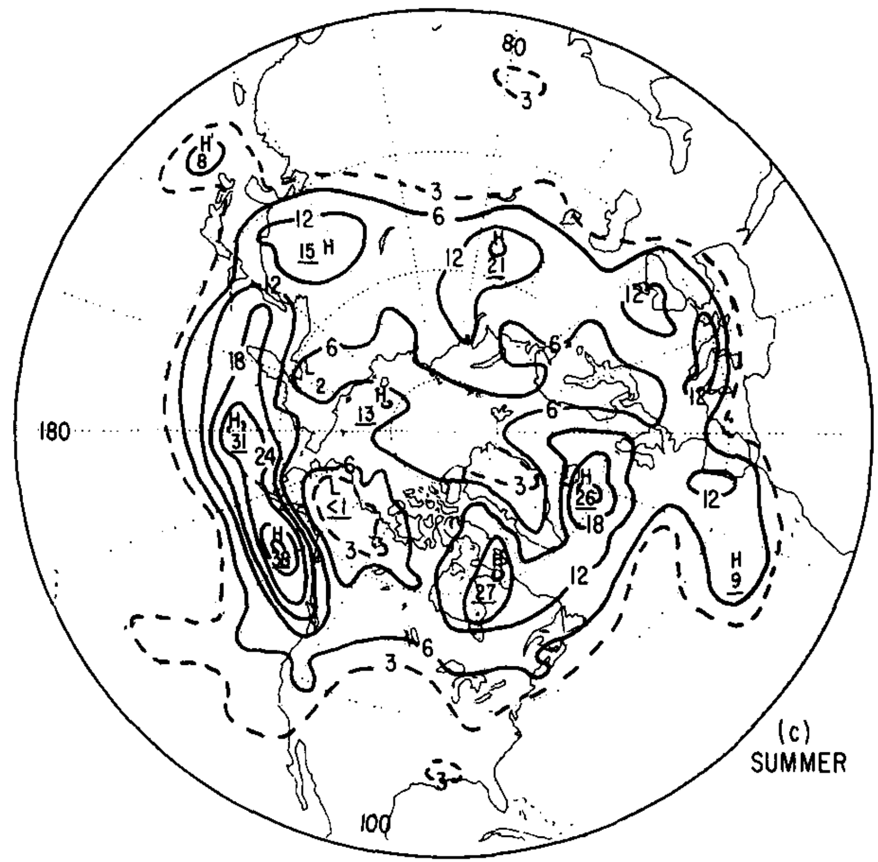

Paper review: Davis, Stoelinga and Kuo (1993), Pomroy and Thorpe (2000), Stoelinga(2003), Thorpe(2003)

direct effect: air parcels pass through maximum $\dot{q}$ and decrease PV above convective region.

indirect effect: negative PV advection by wind field of convection.

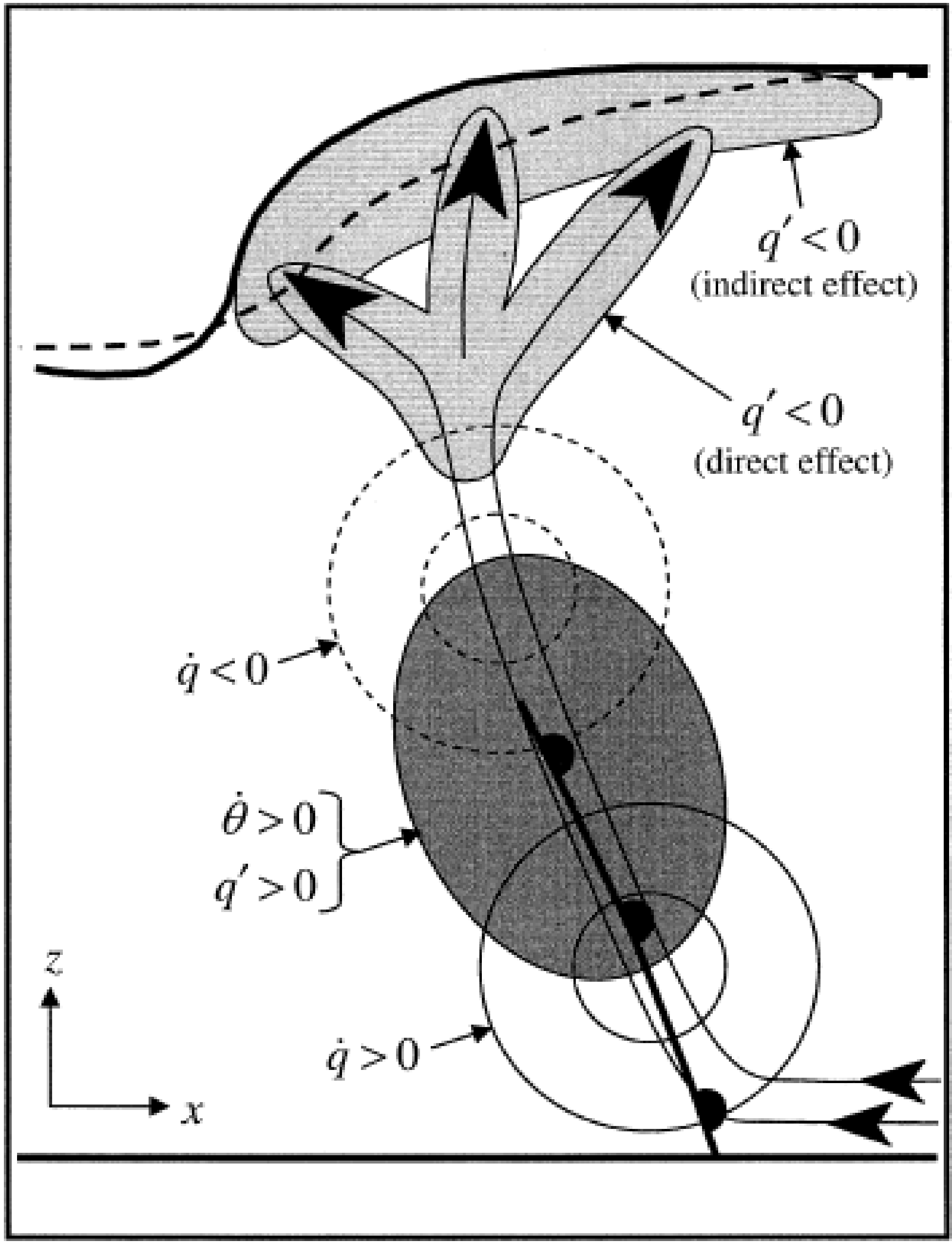

Structural characteristics:

- Kelley & Mock (1982): Palmer type
  1. Composite CCL is confined between 700-100 hPa.
  2. Maximum circulation occurs at 200 hPa.
  3. Cold anomaly is strongest at 300 hPa, and lies north to the vortex center, and weakens gradually toward surface.
  4. Warm anomaly at 125 hPa.
  5. Subsidence and min. cloudiness to NW of CCL, ascent and max. cloudiness to SE of CCL.
  6. Max. vertical motion occurs near 300 hPa.